

Significance of *c.* 300 Ma CHIME zircon age for post-tectonic granite from the Hercynian suture zone, Bamian, Afghanistan

SUZUKI Kazuhiro¹⁾, NAKAI Yutaka²⁾, Daniel J. DUNKLEY¹⁾
and ADACHI Mamoru³⁾

- 1) Nagoya University Center for Chronological Research
- 2) Aichi University of Education
- 3) The Nagoya University Museum

Abstract

CHIME dating was conducted on a sample of massive hornblende-bearing biotite granite collected from a Hercynian suture zone in Bamian, Afghanistan. All zircon grains analyzed exhibit concentric zoning typical of crystallization from a granitic magma. A total of 66 analyses on 12 grains yielded an isochron age of 298+/-28 Ma. This is the first chronological evidence found for the existence of post-tectonic late Carboniferous to early Permian magmatism in the Hercynian suture zone of central Asia, although granitoids of this age are widely recognized in the European Hercynian orogen. This provides a new constraint on the timing and extent of Hercynian orogenesis from Europe to Asia.

Introduction

The Afghanistan territory includes an eastern extension of the Hercynian suture zone, modified by folding caused by the collision of the Indian Plate with the Asian landmass. The complex geology of the area was first investigated through a joint Soviet-Afghan project lasting from 1958 to 1977. The region is interpreted to include (1) a possibly Precambrian basement complex; (2) an Ordovician to lower Devonian passive margin sedimentary succession developed on oceanic crust; (3) an upper Devonian to lower Carboniferous magmatic arc succession; (4) a lower Carboniferous to Permian rift/passive margin sedimentary succession, and (5) a Triassic continental magmatic arc succession beneath Jurassic to Neogene sedimentary rocks (Brockfield and Hashmat, 2001). The stratigraphy of Paleozoic and Mesozoic formations was determined on the basis of index fossils. In contrast, radiometric age data for metamorphic and igneous rocks are scarce. Correlation of metamorphic rocks was carried out solely on the basis of metamorphic grade. Plutonic rocks were divided into Proterozoic, early Carboniferous, Triassic and Meso-Cenozoic intrusions on the basis of intrusive relationships. These estimates, with an absence of late Carboniferous to early Permian plutonism, are in contrast to recent studies which suggest that voluminous granitoids were emplaced into the European Hercynian orogen during post-orogenic extension at around 300 Ma. A question we address in this paper is whether or not similar *c.* 300 Ma granitoids exist in the Hercynian suture zone in Afghanistan.

One of the authors (N.Y.) conducted a broad geologic survey of Afghanistan in 1971. The rock samples collected were put on view at the Nagoya University Museum during the "Afghanistan" exhibition held from November 1, 2002 to January 31, 2003. The samples include hornblende-bearing biotite granite from Bamian, with a K-rich calc-alkaline affinity that is characteristic of

granitoids generated during post-orogenic extension in continent-continent collisions. To determine the emplacement age, CHIME dating of zircon in the hornblende-bearing biotite granite was carried out.

Geological outline

Geological information on Afghanistan was summarized on a 1:2,000,000 map which was published in 1995 by the United Nations Economic and Social Commission for Asia and the Pacific (ESCAP) in cooperation with the Department of Mines and Geological Survey, Ministry of Mines and Industries of Afghanistan. Brockfield and Hashmat (2001) have reported details of the stratigraphy. A simplified tectonic map is shown in Fig. 1. The Harirod strike-slip fault and related faults trend E-W along the Harirod River in central and western Afghanistan, rotate to NE to the north of Kabul, and continue to the Wanch-Akabayatal fault. These fault systems approximate the Hercynian suture line postulated by Burtman and Molnar (1993). The Chaman fault runs NNE–SSW in the southeastern part of Afghanistan and marks the western boundary of the Indian subcontinent (Jadoon and Khushid, 1996).

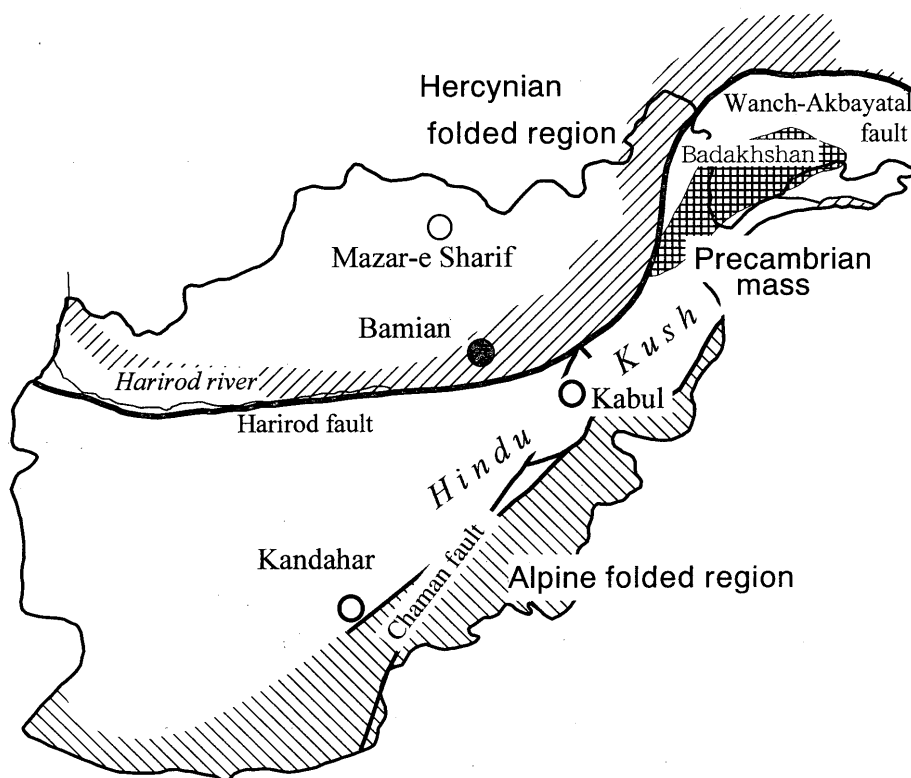


Fig. 1. Map showing major faults and Hercynian and Alpine folded areas in Afghanistan, together with the sampling location (solid circle), Bamian (simplified and modified from Leven, 1997).

Amphibolite to granulite-facies metamorphic rocks in Badakhshan and the Hindu Kush have been correlated to a basement complex in the Pamir Mountains, where 2700–2400 Ma U-Pb isotopic ages were reported (Horeva *et al.*, 1971). Greenschist to amphibolite-facies metamorphic rocks are also developed in a number of districts. These metamorphic rocks were previously assigned to the Proterozoic, but currently they are considered to at least partially represent metamorphosed Ordovician to lower Devonian passive margin successions, due to the presence of ophiolitic me-

langes that include greenschist, blueschist, radiolarian chert, metabasalt, metagabbro and serpentinite.

Metamorphic rocks from Bamian to the western Hindu Kush are overlain by basal conglomerates containing unmetamorphosed Visean limestone pebbles, as well as clasts of metasedimentary, acid volcanic and plutonic rocks (Blaise *et al.*, 1993). The conglomerates grade upwards into Permian (Artinskian to Murgabian) limestones. All these lithologies are unconformably overlain by Triassic intermediate to acid volcanics and volcanoclastic sediments, which represent a continental magmatic arc succession.

Granitoids with assumed Proterozoic ages occur as sub-conformable bodies associated with high-grade metamorphic rocks in northeastern Afghanistan (Fig. 1). Discordant granitoids intrude metamorphic rocks in northeastern Badakhshan and the western Hindu Kush and have been regarded as early Carboniferous in age, as some bodies are overlain by middle to upper Carboniferous formations. Large batholiths in the western Hindu Kush are regarded as post-Triassic in age, as some intrude Triassic volcanic units and volcanoclastic sediments (Boulin, 1988). The batholiths comprise I-type granitoids with Rb-Sr isochron ages of *c.* 210 Ma and S-type granitoids of *c.* 190 Ma (Debon *et al.*, 1987). Plutonic and volcanic complexes that occur along the Chaman fault belong to an Alpine magmatic cycle that began in the late Jurassic. No Permo-Carboniferous granitoids have been reported from the Hercynian fold belt in Afghanistan.

Sample Description

The sample was collected from a granitic pluton north of the Harirod fault, Bamian. According to the 1:2,000,000 geologic map, the pluton intrudes an undifferentiated lower Carboniferous formation, and is covered by Maastrichtian to Paleogene sediments. The sample is of coarse-grained hornblende-bearing biotite granite and has no foliation. It consists mainly of quartz, plagioclase and microcline with lesser amounts of biotite and hornblende. Accessory minerals include allanite, apatite, and zircon. Iron oxides or titanite were observed under the microscope. An XRF analysis of the sample is given in Table 1. The sample has a calc-alkaline composition with moderately high (4.07 %) K₂O, and falls within the high-K calc-alkaline field of Barbarin (1999).

Quartz grains, mostly 1–3 mm in size, show little undulatory extinction. Microcline contains perthitic blebs that constitute a substantial proportion of individual grains. Plagioclase is partially saussuritized or sericitized. Oscillatory zoning is marked by unaltered portions of oligoclase and distinct boundaries of saussuritized and sericitized areas (Fig. 2). Biotite is present with a pleochroism of X= straw yellow and Y= dark brown, and is partially altered to green chlorite. Hornblende is also present, with X= pale yellow green, Y= brownish green and Z= bluish green.

Table 1. XRF analysis of hornblende-bearing biotite granite from Bamian, Afghanistan

SiO ₂	73.38	Quartz	31.85
TiO ₂	0.28	Corundum	0.18
Al ₂ O ₃	12.89	Orthoclase	24.05
Σ Fe as FeO	2.43	Albite	29.36
MnO	0.06	Anorthite	7.08
MgO	0.56	Hypersthene	5.50
CaO	1.52	Ilmenite	0.53
Na ₂ O	3.47	Apatite	0.16
K ₂ O	4.07		
P ₂ O ₅	0.07		
Total	98.73		

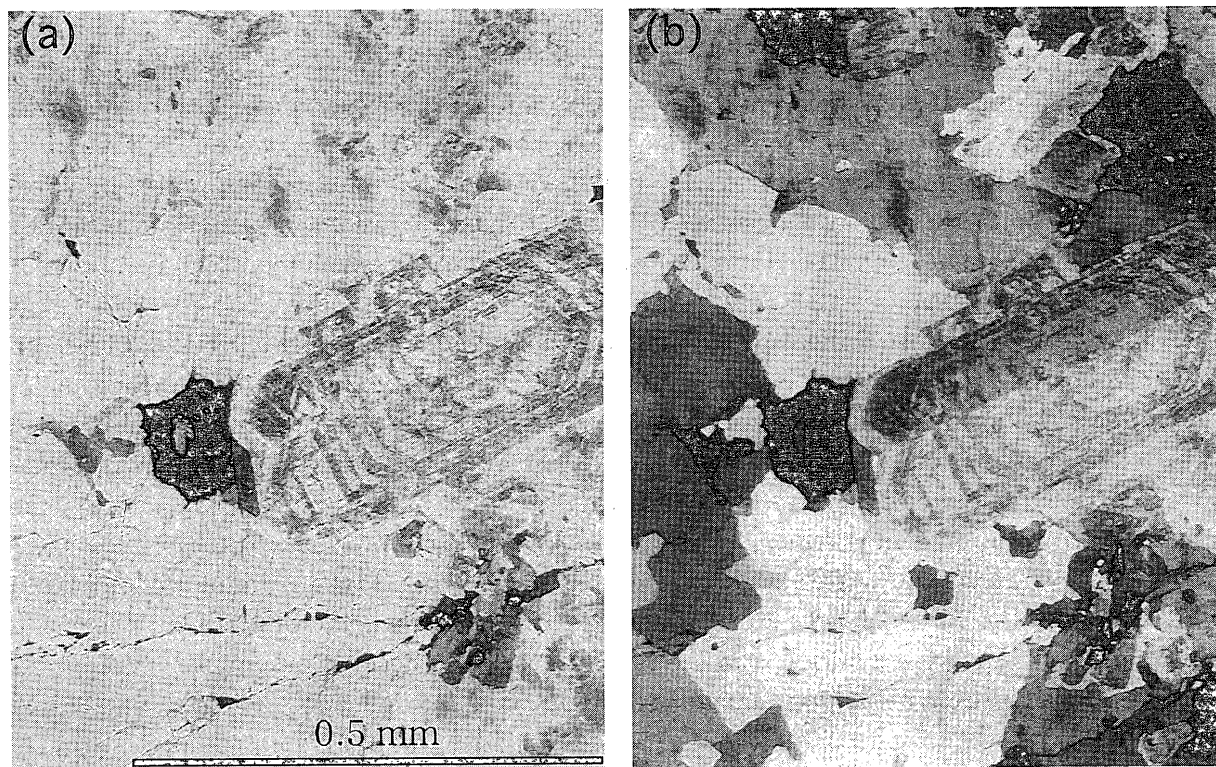


Fig. 2. Photomicrographs of hornblende-bearing biotite granite from Bamian, one polarized light (a) and crossed polars (b). Distinct boundaries between unaltered zones and saussuritized and sericitized zones mark oscillatory zoning of plagioclase.

Allanite and zircon occur mainly in close association with biotite, and sometimes as inclusions. Allanite is pleochroic from deep reddish brown to pale brown. Most grains are homogeneous, but some have deep brown centers and pale brown margins. A preliminary analysis suggests that allanite grains, especially the deep-colored centers, contain significant amounts (*c.* 0.2 wt.%) of Pb but a limited range of ThO₂ (1.5–3.8 wt.%). Allanite, therefore, was not used for the CHIME dating. Zircon occurs as faceted prisms 0.05–0.3 mm in length, with concentric zoning. Most zircon grains are transparent and colorless under the microscope, but some portions of U-enriched grains are metamict.

Zircon grains in conventional polished thin sections were analyzed on a Jeol JCSA-733 electron microprobe at the Nagoya University Center for Chronological Research. For analytical techniques and data reduction methods, readers should refer to Suzuki and Adachi (1991, 1994 and 1998).

Results and Discussion

A total of 123 spots on 12 zircon grains were analyzed (Table 2). The ThO₂ contents range from less than the detection limit (0.005 wt.%) to 0.528 wt.%, and UO₂ contents from 0.021 wt.% to 1.02 wt.%. Of these, only 67 spots contain measurable amounts (>0.004 wt.%) of PbO. The analytical data are plotted on a PbO vs. UO₂* diagram (Fig. 3) following the CHIME method of Suzuki and Adachi (1991). All data points, except a highly uraniferous datum (UO₂=1.02 wt.%) from grain Z02, define an isochron of 298±28 Ma (MSWD=0.71) with an intercept value of -0.003±-0.0008. Since the isochron is well defined and passes through the origin, the CHIME zircon age is reliable. The concentric zoning and euhedral morphology of individual grains indicate that the zircon crystals were formed in a magma chamber (Hanchar and Miller, 1993). The mea-

Table 2. Electron microprobe analyses of ThO₂, UO₂ and PbO in zircon from hornblende-bearing biotite granite from Bamian, Afghanistan. UO₂* represents sum of the measured UO₂ and UO₂ equivalent of the measured ThO₂.

Spot	X	Y	ThO ₂	UO ₂	PbO	Ma	UO ₂ *	Spot	X	Y	ThO ₂	UO ₂	PbO	Ma	UO ₂ *
Z01	623, 647		0.052	0.089	—	—	—	Z05	316, 752		0.040	0.088	—	—	—
Z01	631, 652		0.152	0.189	0.0094	292	0.236	Z05	316, 758		0.071	0.115	0.0065	347	0.136
Z01	623, 652		0.058	0.118	0.0046	250	0.136	Z05	316, 766		0.045	0.050	—	—	—
Z01	616, 652		0.055	0.091	0.0042	286	0.108	Z05	322, 747		0.081	0.167	0.0107	404	0.192
Z01	612, 658		0.117	0.135	0.0053	228	0.171	Z05	322, 754		0.026	0.074	—	—	—
Z01	617, 658		0.050	0.108	—	—	—	Z05	322, 761		0.043	0.098	—	—	—
Z01	623, 658		0.084	0.131	0.0063	294	0.157	Z05	322, 768		0.065	0.129	—	—	—
Z01	629, 658		0.048	0.105	—	—	—	Z05	331, 747		0.043	0.057	—	—	—
Z01	626, 662		0.044	0.076	—	—	—	Z05	331, 760		0.033	0.055	—	—	—
Z01	626, 656		0.045	0.076	—	—	—	Z05	336, 754		0.074	0.115	0.0072	380	0.138
Z02	822, 063		0.032	0.185	0.0053	201	0.195	Z06	686, 854		0.065	0.117	0.0049	262	0.137
Z02	829, 063		0.034	0.197	0.0090	318	0.207	Z06	692, 854		0.170	0.260	0.0093	219	0.313
Z02	818, 068		0.138	0.339	0.0157	301	0.382	Z06	698, 854		0.198	0.282	0.0136	291	0.342
Z02	823, 068		0.093	0.271	0.0114	279	0.299	Z06	702, 859		0.069	0.135	—	—	—
Z02	829, 068		0.043	0.172	0.0078	308	0.185	Z06	694, 859		0.060	0.142	0.0082	371	0.161
Z02	847, 068		0.035	0.190	0.0108	391	0.200	Z06	686, 859		0.073	0.150	0.0074	313	0.173
Z02	853, 068		0.041	0.240	0.0076	222	0.253	Z06	688, 866		0.068	0.134	0.0064	301	0.155
Z02	857, 075		0.031	0.195	0.0073	263	0.204	Z06	695, 866		—	0.102	—	—	—
Z02	850, 075		0.027	0.139	0.0050	250	0.147	Z06	703, 866		0.063	0.109	—	—	—
Z02	828, 075		0.108	0.234	0.0099	272	0.267	Z06	707, 872		0.052	0.085	—	—	—
Z02	830, 083		0.074	0.207	0.0095	303	0.229	Z07	946, 007		0.082	0.170	0.0088	329	0.195
Z02	846, 083		0.065	0.243	0.0106	296	0.263	Z07	948, 017		0.054	0.111	—	—	—
Z02	843, 089		0.169	1.02	0.0194	134	1.08	Z07	943, 017		0.037	0.090	—	—	—
Z02	830, 089		0.082	0.233	0.0099	281	0.258	Z07	955, 025		0.068	0.148	0.0052	226	0.170
Z02	824, 092		0.051	0.182	0.0105	386	0.197	Z07	948, 025		0.047	0.104	—	—	—
Z03	305, 112		0.119	0.216	0.0066	193	0.253	Z07	938, 025		0.063	0.101	—	—	—
Z03	305, 121		0.075	0.126	0.0070	342	0.149	Z07	958, 039		0.039	0.091	—	—	—
Z03	311, 105		0.062	0.116	0.0066	356	0.135	Z07	948, 039		0.050	0.083	—	—	—
Z03	311, 115		0.031	0.060	—	—	—	Z07	935, 039		0.058	0.171	0.0053	207	0.189
Z03	311, 123		0.046	0.090	—	—	—	Z07	915, 039		0.039	0.134	0.0059	296	0.146
Z03	311, 128		0.053	0.126	0.0059	303	0.142	Z07	947, 054		0.053	0.091	—	—	—
Z03	319, 102		0.228	0.417	0.0201	302	0.487	Z07	935, 054		0.052	0.088	—	—	—
Z03	319, 112		0.154	0.307	0.0168	346	0.354	Z07	920, 054		0.064	0.120	—	—	—
Z03	319, 124		0.061	0.187	0.0108	382	0.205	Z07	900, 054		0.104	0.188	0.0056	188	0.221
Z03	319, 133		0.038	0.065	—	—	—	Z07	904, 065		0.081	0.170	0.0102	382	0.194
Z03	330, 089		0.027	0.055	—	—	—	Z07	915, 065		0.046	0.083	—	—	—
Z03	330, 099		0.059	0.062	—	—	—	Z07	934, 065		0.039	0.081	—	—	—
Z03	330, 132		0.061	0.190	0.0078	274	0.209	Z07	922, 080		0.030	0.094	—	—	—
Z03	330, 143		0.044	0.050	—	—	—	Z07	922, 054		0.072	0.126	—	—	—
Z03	342, 085		0.067	0.139	0.0060	275	0.160	Z07	943, 029		0.057	0.104	—	—	—
Z03	342, 098		0.081	0.100	—	—	—	Z08	330, 902		0.032	0.042	—	—	—
Z03	342, 107		0.360	0.544	0.0278	311	0.654	Z08	303, 902		0.333	0.267	0.0174	344	0.369
Z03	342, 119		0.149	0.339	0.0162	308	0.385	Z08	297, 894		0.202	0.193	0.0113	324	0.255
Z03	353, 103		0.436	0.619	0.0314	305	0.753	Z08	303, 894		0.290	0.236	0.0155	347	0.325
Z03	353, 117		0.234	0.424	0.0196	290	0.496	Z08	303, 910		0.252	0.223	0.0114	278	0.301
Z03	353, 129		0.070	0.180	0.0086	312	0.201	Z08	330, 910		0.017	0.021	—	—	—
Z03	353, 137		0.054	0.147	0.0077	342	0.164	Z08	337, 910		0.038	0.068	—	—	—
Z03	364, 095		0.042	0.076	—	—	—	Z08	337, 922		0.051	0.073	—	—	—
Z03	377, 118		0.528	0.519	0.0240	259	0.681	Z08	330, 922		0.033	0.041	—	—	—
Z03	377, 129		0.060	0.132	0.0053	259	0.150	Z08	321, 927		0.051	0.038	—	—	—
Z03	392, 097		0.048	0.086	—	—	—	Z09	009, 825		0.528	0.220	0.0161	308	0.382
Z03	392, 109		0.038	0.050	—	—	—	Z10	731, 336		0.196	0.275	0.0156	339	0.335
Z03	392, 121		0.030	0.045	—	—	—	Z11	171, 431		0.055	0.105	—	—	—
Z03	386, 123		0.034	0.069	—	—	—	Z11	177, 429		0.045	0.113	—	—	—
Z04	095, 802		0.062	0.100	0.0048	296	0.119	Z11	179, 423		0.024	0.051	—	—	—
Z04	105, 802		0.100	0.138	0.0062	270	0.169	Z11	109, 485		0.171	0.287	0.0155	333	0.339
Z04	113, 802		0.080	0.119	0.0083	417	0.144	Z11	115, 489		0.114	0.403	0.0194	324	0.437
Z04	117, 809		0.059	0.088	—	—	—	Z11	119, 491		0.182	0.368	0.0160	277	0.424
Z04	109, 809		0.079	0.167	0.0084	321	0.191	Z12	768, 033		0.343	0.308	0.0154	273	0.414
Z04	100, 809		0.059	0.108	—	—	—								
Z04	100, 817		0.108	0.193	0.0090	292	0.226								
Z04	113, 817		0.073	0.107	—	—	—								
Z04	119, 817		0.046	0.061	—	—	—								
Z04	103, 821		0.052	0.092	—	—	—								

sured age of 298 ± 28 Ma is therefore regarded as the emplacement time of the hornblende-bearing biotite granite.

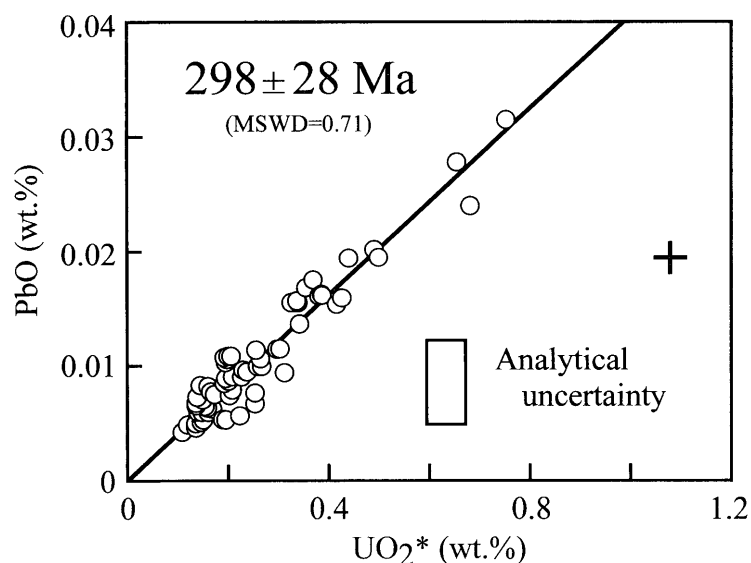


Fig. 3. Plot of PbO vs. UO_2^* of zircon grains. Cross is a data point (1.02 wt. % UO_2 and 134 Ma apparent age) that is not included in the CHIME age calculation. The error box in the figure represents 2σ analytical uncertainty, and error given to age is of 2σ .

The 298 ± 28 Ma age corresponds to the Stephanian stage of Carboniferous according to Harland *et al.* (1990). The new age does not correspond to previously assigned ages for Hercynian plutonism in Afghanistan. Instead, it may characterize a magmatic episode related to post-thickening collapse in the Hercynian orogen. Recognized events in the European Hercynian orogen include a final ductile deformation phase during the Namurian and Westphalian stages, followed by brittle deformation phase in the Permian (Pereira *et al.*, 1993). These deformation phases represent post-thickening extension tectonics that followed the Hercynian continent-continent collision in the middle Carboniferous (Faure and Becq-Giraudon, 1993). After the ductile deformation stage, large volumes of granitoids were emplaced into the European Hercynian orogen within a short time range (*e.g.* Dias *et al.*, 1998; Almeida *et al.*, 1998; Alexandrova *et al.*, 2000; Morillona *et al.*, 2000). The plutonism is characterized by a predominance of K-rich calc-alkaline granitoids (*e.g.* Rottura *et al.*, 1998; Silva *et al.*, 2000). The present study suggests that K-rich calc-alkaline magmatism related to the post-thickening extension is contemporaneous throughout the Hercynian orogen from Europe to Asia.

Acknowledgements

The authors would like to thank S. Yogo for his assistance in sample preparation, T. Kato and K. Tsukada for technical assistance and helpful discussions and K. Wakita for providing geological information of Afghanistan.

References

- Alexandrova, P., Cheilletza, A., Deloulea, E. and Cuney, M. (2000) 319 ± 7 Ma crystallization age for the Blond granite (northwest Limousin, French Massif Central) obtained by U/Pb ion-probe dating of zircons. *G. R. Acad. Sci., Paris, II*, **330**, 617-622.

- Almeida, A., Leterrier, J., Noronha, P. and Bertrand, J.M. (1998) U-Pb zircon and monazite geochronology of the Hercynian two-mica granite composite pluton of Cabeceiras de Basto (Northern Portugal). *G. R. Acad. Sci., Paris, II*, **326**, 779-785.
- Barbarin, B. (1999) A review of the relationships between granitoid types, their origins and their geodynamic environments. *Lithos*, **46**, 605-626.
- Blaise, J., Boulin, J., Bouyx, E., Lardeuax, H. and Vachard, D. (1993) Identification de faunes devoniennes dans les formations metamorphiques de L'Hindu Kouch occidental, en Afghanistan: implications. *G. R. Acad. Sci., Paris, II*, **317**, 963-969.
- Boulin, J. (1988) Hercynian and Eocimmerian events in Afghanistan and adjoining regions. *Tectonophysics*, **148**, 253-278.
- Brookfield, M.E. and Hashmat, A. (2001) The geology and petroleum potential of the North Afghan platform and adjacent areas (northern Afghanistan, with parts of southern Turkmenistan, Uzbekistan and Tajikistan). *Earth Sci. Rev.*, **55**, 41-71.
- Burtman, V.S. and Molnar, P. (1993) Geological and geophysical evidence for deep subduction of continental crust beneath the Pamir. *Geol. Soc. Am. Sec. Pap.* 281, 76pp.
- Debon, F., Afzali, H., FeFort, P., Sonet, J. and Zimmrtmann, J.L. (1987) Plutonic rocks and associations in Afghanistan: typology, age and geodynamics setting. *Memoire Science de la Terre, Nancy*, **49**, 132pp.
- Dias, G., Leterrier, J., Mendes, A., Simões, P.P. and Bertrand, J.M. (1998) U-Pb zircon and monazite geochronology of post-collisional Hercynian granitoids from the Central Iberian Zone (Northern Portugal). *Lithos*, **45**, 349-369.
- Faure, M. and Becq-Giraudon, J.F. (1993) Sur la succession des episodés extensifs au cours du desepaississement carbonifere du Massif central franeais. *G. R. Acad. Sci., Paris, II*, **110**, 967-973.
- Harland, W.B., Armstrong, R.L., Cox, A.V., Craig, L.E., Smith, A.G. and Smith, D.G. (1990) A geologic time scale 1989. Cambridge University Press, 262 pp.
- Hanchar, J.M. and Miller, C.F. (1993) Zircon zonation patterns revealed by cathodoluminescence and back-scattered electron images: implications for interpretation of complex crustal histories. *Chem. Geol.*, **303**, 1-13.
- Horeva, B.Ja., Iskanderova, A.D., Shergina, Ju.P. (1971) Age of protoliths from metamorphic series of SW Pamir, according to the Pb isotope method. *Izvestia AN SSSR, ser. Geologicheskaya*, **8**, 40-46 (in Russian).
- Jadoon, I.A.K. and Khushid, A. (1996) Gravity and tectonic model across the Sulaiman fold belt and the Chaman fault zone in western Pakistan and eastern Afghanistan. *Tectonophysics*, **254**, 89-109.
- Leven, E.Ja. (1997) Permian stratigraphy and Fusulinida of Afghanistan with their paleogeographic and paleotectonic implications (translated by T. Yu. Shalashina, edited by C.H. Stevens and D.L. Baars). *Geol. Soc. Am. Sec. Pap.* 316, 134pp.
- Morillona, A.C., Feraud, G., Sosson, M., Ruffet, G., Crevola, G. and Lerouge, G. (2000) Diachronous cooling on both sides of a major strike-slip fault in the Variscan Maures Massif (south-east France), as deduced from a detailed $^{40}\text{Ar}/^{39}\text{Ar}$ study. *Tectonophysics*, **321**, 103-126.
- Pereira E., Ribeiro, A and Meireles, C. (1993) Cisalhamentos hercnicos e controlo das mineralizacoes de Sn-W, Au e U na Zona Centro-Iberica, em Portugal. *Cuad. Lab. Xeol. Laxe*, **19**, 89-119.
- Rottura, A., Bargossi, G.M., Gaggianelli, A., Del Moro, A., Vison, D. and Tranne, C.A. (1998) Origin and significance of the Permian high-K calc-alkaline magmatism in the central-eastern Southern Alps, Italy. *Lithos*, **45**, 329-348.
- Silva, M.M.V.G., Neiva, A.M.R. and Whitehouse, M.J. (2000) Geochemistry of enclaves and host granites from the Nelas area, central Portugal, *Lithos*, **50**, 153-170.
- Suzuki, K. and Adachi, M. (1991) Precambrian provenance and Silurian metamorphism of the Tsubonosawa paragneiss in the South Kitakami terrane, Northeast Japan, revealed by the chemical Th-U-total Pb isochron ages of monazite, zircon and xenotime. *Geochemical J.*, **25**, 357-376.
- Suzuki, K. and Adachi, M. (1994) Middle Precambrian detrital monazite and zircon from the Hida gneiss in the Oki-Dogo Island, Japan: their origin and implication for the correlation of the basement gneiss of Southwest Japan and Korea. *Tectonophysics*, **235**, 277-292.
- Suzuki, K. and Adachi, M. (1998) Denudation history of the high T/P Ryoke metamorphic belt, Southwest Japan: constraints from CHIME monazite ages of gneisses and granitoids. *J. metamorphic Geol.*, **16**, 23-37.